MADRID
inter.noise 2019
June 16 - 19
NOISE CONTROL FOR A BETTER ENVIRONMENT

Study on Coordinated Control Strategy of Electric Vehicle AFS and DYC Based on Phase Plane Method

Liang Xiutian[1], Chen Wuwei[1+], Hu Yanping[1], Xu Yong[2], Wang Xiao[1]
1. School of Automotive and Transportation Engineering, Hefei University of Technology, Hefei 230009, China
2. School of Mechanical Engineering, Anhui Institute of Information Technology, Wuhu 241000, China

ABSTRACT

In order to improve the path tracking ability and dynamic stability of a four in-wheel-motors drive electric vehicle, the dynamic models of the vehicle are built and the boundary of the dynamic stability range is determined by using phase plane method. Then, the layered control structure is adopted for designing a control system. The upper layer controller adopts the extension coordination control method to determine the weights of the active front-wheel steering (AFS) controller and the direct yaw-moment controller (DYC). The middle layer controller uses the nonlinear triple-step control method to calculate the additional front-wheel angle and the additional yaw-moment required by the vehicle. The switching control of the active front-wheel steering controller and the direct yaw-moment controller is realized according to the dynamic stability and riding state of the vehicle. At the lower layer controller, two signals obtained by the upper layer controller are used to optimize the four driving motor torques based on the quadratic programming method. These signals are the additional front-wheel angle and additional yaw-moment, and they are delivered to the steering motor and four driving in-wheel-motors. The model and controller of the in-wheel-motor driving vehicle are built by CarSim and MATLAB/Simulink software, and the simulation analysis is carried out under the double-lane change condition. The results show that the proposed vehicle controller strategy can improve the path tracking ability and the dynamic stability of the whole vehicle. And the riding vibration of the electric vehicle is also improved.

Key words: in-wheel-motor, extension coordination control, dynamic stability
I-INCE Classification of Subject Number: 00

[1] xtl0094@163.com
[1+] hfgdcjs@126.com

1. INTRODUCTION

Nowadays, with the number of cars continues to increase, fuel vehicles consume a large amount of fossil fuels, and exhaust emissions, the high energy consumption and environmental pollution have become the focus of global attention. As a kind of the environment-friendly and resource-saving transportation means, electric vehicles (EV) are widely recognized as one of the solutions to today's environmental pollution and energy shortage. Compared with conventional fuel vehicles, in-wheel-motor drive electric vehicle have higher control accuracy and faster response speed. The driving torque of four wheels can be independently controlled, which can improve the vehicle's stability and maneuverability. In reference [1], a kind of controller was designed based on a two-DOF vehicle model, the weight functions of the active front-wheel steering (AFS) control and direct yaw-moment control (ESC) are given. The simulation results show that the controller has good robustness for the dynamic steering of the electric vehicles. Literature [2] designed an active front-wheel steering system (AFS) and a dynamic integrated control system (DIC). When the braking and steering system are coupled, the DIC can compensate and improve the performance of the AFS. The experimental results show that the AFS has good performance in terms of steering assisting and motion stabilization, and the integrated dynamic control system improves the lateral stability of the vehicle. In reference[3], a global optimization algorithm for anti-disturbance is proposed to solve the torque distribution problem of a in-wheel-motor drive EV. The driver's expected traction and the direct yaw-moment are calculated by the driver model and direct yaw-moment control strategy respectively. The nonlinear objective function of the vehicle stability is established based on the constraint of wheel adhesion limit, then the objective function is transformed into the eigenvalue problem. In reference [4], an improved nonlinear compounded feedback controller is designed for a in-wheel-motor drive EV path tracking, and the dynamic curvature of the desired path is given. The path tracking is realized through the combination control of lateral and yaw motion. The simulation results show that the controller can improve the transient response performance and eliminate steady-state error effectively. Literature [5] designed an integrated controller of the AFS and the DYC for the boundary control of a four-wheel drive vehicle which is used to track the desired path within a restricted safety range. The speed controller calculates required traction and yaw moment. In the path tracking controller, a feedforward-feedback lateral motion controller is designed to calculate the desired steering-angle to follow the desired path. The phase plane method is used to determine the control boundary.

In this paper, the extension coordination control strategy for the AFS and the DYC is proposed based on the stability control of a in-wheel-motor drive EV. Here, a hierarchical control structure is designed, and the weights of the AFS and the DYC controllers are calculated by using the extension coordination control strategy in the upper layer control system. In the middle layer control system, the AFS and the DYC controllers are designed based on the nonlinear triple-step method. In the lower layer control system, the total driving torque and the additional yaw-moment are optimally distributed to the four wheels based on the pseudo-inverse optimization algorithm. Thus, the theory analysis, simulation, hardware-in-the-loop tests and vehicle running experiments are carried out. The results show that the proposed control strategy can effectively improve the dynamic stability of the vehicle. And the riding vibration of the electric vehicle is also improved.

2. DYNAMIC MODELING of THE In-wheel-motor DRIVE EV

2.1 Vehicle Dynamic Modeling

(1) 3-DOF Vehicle Model

The stability of EV is mainly determined by the lateral motion and yaw motion. The vehicle model is shown in Fig. 1, considering the longitudinal motion along the x-axis direction, the lateral motion along the y-axis direction and the yaw motion around the z-axis. The model contains three degrees of freedom, it is simplified and assumed as follows: Ignore external factors such as wind resistance and road bump; ignore the vehicle pitch and roll angles; assume the front and rear wheel tracks are equal and the mechanical properties of tires are the same; and also assume the front-wheel steering angles are equal[6].

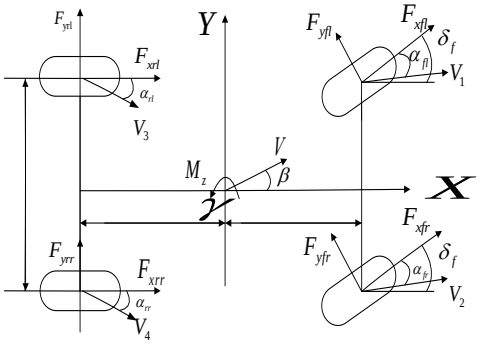

Fig.1. *3–DOF Vehicle model*

The motion equation of the vehicle is:

$$\begin{cases} m\left(\dot{v}_x - v_y\gamma\right) = \left(F_{xfl} + F_{xfr}\right)\cos\delta_f + F_{xrl} + F_{xrr} - \left(F_{yfl} + F_{yfr}\right)\sin\delta_f \\ m\left(\dot{v}_y + v_x\gamma\right) = \left(F_{yfl} + F_{yfr}\right)\cos\delta_f + F_{yrl} + F_{yrr} + \left(F_{xfl} + F_{xfr}\right)\sin\delta_f \\ I_z\dot{\gamma} = l_f\left(F_{yfl} + F_{yfr}\right)\cos\delta_f + l_f\left(F_{xfl} + F_{xfr}\right)\sin\delta_f - l_r\left(F_{yrl} + F_{yrr}\right) - \\ \frac{\mathrm{d}}{2}\left(F_{xfl} - F_{xfr}\right)\cos\delta_f + \frac{d}{2}\left(F_{yfl} - F_{yfr}\right)\sin\delta_f - \frac{d}{2}\left(F_{xrl} - F_{xrr}\right) \end{cases} \tag{1}$$

where m is the complete vehicle mass, v_x is the longitudinal speed along the x-axis, $\dot{v}_x$ is the longitudinal acceleration, v_y is the lateral speed along the y-axis, $\dot{v}_y$ is the lateral acceleration, γ is the yaw rate, $\dot{\gamma}$ is the yaw acceleration, F_{xi} and F_{yi} are the longitudinal and lateral forces of the tire respectively ($i = (fl, fr, rl, rr)$, I_z is the moment of inertia around the z-axis, l_f and l_r are the distance from the mass center to the front and rear axes respectively, d is the wheel track, δ_f is the front-wheel steering angle.

(2) Dynamic model of the in-wheel-motor

A single-wheel driving model is often used when analyzing the dynamic performance of wheel driving. Ignoring the frictional resistance, the equation is expressed as:

$$J_\omega\dot{\omega}_i = T_{di} - F_{xi}R, i = \left(fl, fr, rl, rr\right) \tag{2}$$

where J_ω is the wheel moment of inertia, $\dot{\omega}_i$ is the angular acceleration of the wheel, T_{di} is the output torque of the motor, R is the wheel rolling radius.

This paper focuses on the stability control strategy of the EV, and the in-wheel-motor is a permanent magnet synchronous motor with a very fast response speed. Therefore, the motor model is simplified as a second-order system; that is, the transfer function of

the electro- magnetic actual torque and the target torque is as follows[7]:

$$\frac{T_d}{T_d^*} = \frac{1}{2\xi^2 s^2 + 2\xi s + 1} \tag{3}$$

where T_d is the actual torque of the motor, T_d^* is the target torque required for stability control, ξ is determined by the motor parameters.

(3) Tire Model

Tire model is very important for the study of wheel dynamics. Because magic formula tire model has good generality, the model is used in this paper, and the expression is as follows[6]:

$$\begin{cases} y(x) = D\sin\left\{C\arctan\left[Bx - E(Bx - \arctan(Bx))\right]\right\} \\ Y(x) = y(x) + S_v \\ x = X + S_h \end{cases} \tag{4}$$

where $Y(x)$ is the lateral force or longitudinal force, X is the side-slip angle or longitudinal slip ratio of the tire, B, C, D and E are calculated by the vertical load and the camber angle of the tire.

(4) Driver Model

Here, the driver model of single-point preview is used for path tracking. The block diagram is shown in Figure 2. The input is the deviation at the preview point, and the output is the steering-wheel angle[8].

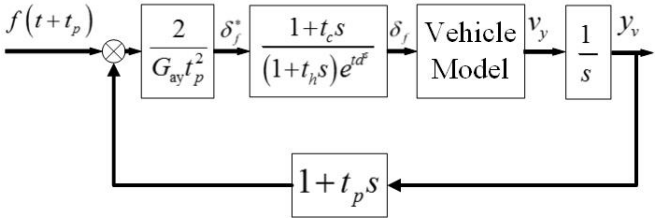

Fig.2. *Driver model*

where f is the desired lateral displacement, y_v is the actual lateral displacement, t_p is the preview time, t_d is the driver response lag time, δ_f^* is the desired front-wheel steering angle, δ_f is the actual front-wheel steering angle, G_{ay} is the steady state gain of the vehicle lateral acceleration to the front-wheel steering angle.

Among them:

$$G_{ay} = \frac{v_x^2}{L\left(1 + Kv_x^2\right)} \tag{5}$$

where L ($L=l_f + l_r$) is the wheel base of the vehicle, K is the stability factor which is related to the vehicle parameters, i.e:

$$K = \frac{m(l_r C_r - l_f C_f)}{2L^2 C_r C_f} \tag{6}$$

where C_f, C_r are the cornering stiffness of the front and rear tires.

2.2 2-DOF Reference Model

Here, a 2-DOF model is selected as the reference model to obtain the ideal yaw rate and sid-slip angle required for stability control[9]. The ideal yaw rate γ^* and side-slip angle of vehicle mass-center, β^*, are available:

$$\begin{cases} \gamma^* = \min\left\{\dfrac{v_x\delta_f}{l\left(1+Kv_x^2\right)}, \dfrac{\mu g}{v_x}\right\} \\ \beta^* = \min\left\{\left(\dfrac{l_r}{v_x^2}+\dfrac{ml_f}{2C_rL}\right)\dfrac{v_x^2}{L\left(1+Kv_x^2\right)}\delta_f, \mu g\left(\dfrac{l_r}{v_x^2}+\dfrac{ml_f}{2C_rl}\right), \beta_1\right\} \end{cases} \tag{7}$$

where $\beta_1 = \pm 2^\circ$ is the critical value of the road with low adhesion coefficient, $\beta_1 = \pm 10^\circ$ is the critical value of the road with high adhesion coefficient, μ is the road adhesion coefficient.

3. Control System Design

3.1 Determination of the Stability Domain Boundary

(1) Stability Domain Boundary Solving Method

The division of the stability domain boundary based on the phase plane mainly includes the two-line method, the double-fold method, the five-eigenvalue diamond method and the limit cycle method, etc.

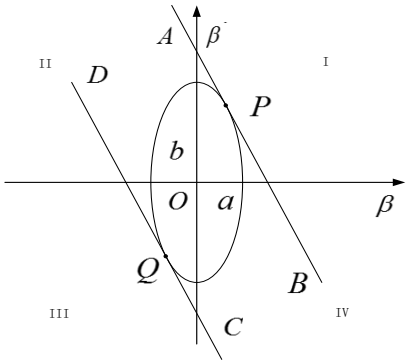

Fig.3 *Boundary of phase plane stability domain*

Figure 3 shows the boundary of phase plane stability domain. In the figure, the straight lines AB and CD are the boundary lines of the phase plane stability domain of the two-line method, AB and CD are expressed as:

$$\left|c_1\beta + c_2\dot{\beta}\right| \le 1 \tag{8}$$

where C_1 nd C_2 are constants and are determined by vehicle parameters.

The $\beta - \dot{\beta}$ limit cycle method considers that the stability domain boundary of the vehicle is elliptical, the interior of the elliptic is the stable domain, and the exterior is the unstable domain. The elliptic equation can be expressed as:

$$\left(\frac{\beta}{a}\right)^2 + \left(\frac{\dot{\beta}}{b}\right)^2 = 1 \tag{9}$$

The elliptic boundary is tangent to the line AB and the line CD, and the following equations are obtained:

$$\begin{cases} \left(\dfrac{\beta}{a}\right)^2 + \left(\dfrac{\dot{\beta}}{b}\right)^2 = 1 \\ c_1\beta + c_2\dot{\beta} - 1 = 0 \end{cases} \tag{10}$$

$$\begin{cases} \left(\frac{\beta}{a}\right)^2 + \left(\frac{\dot{\beta}}{b}\right)^2 = 1 \\ c_1\beta + c_2\dot{\beta} + 1 = 0 \end{cases} \tag{11}$$

Solving equations(10), (11), then the following equation can be obtained:

$$c_1^{\ 2}a^2 + c_2^{\ 2}b^2 = 1 \tag{12}$$

(2) Determination of $\beta - \dot{\beta}$ Stability Domain Boundary

During the vehicle driving, the boundary of the phase plane stability domain is affected by the vehicle speed, the road adhesion coefficient and the front-wheel steering angle. Therefore, the effect of three factors on the phase plane boundary should be analyzed firstly.

1) Effect of speed on phase plane boundary

The road adhesion coefficient is 0.9 and remains unchanged, and the front-wheel steering angle is 0^o and remains unchanged. The speed ranges from 130km/h to 30km/h and the limit cycle method was used to plot the stability domain boundary at each speed, as shown in Figure 4.

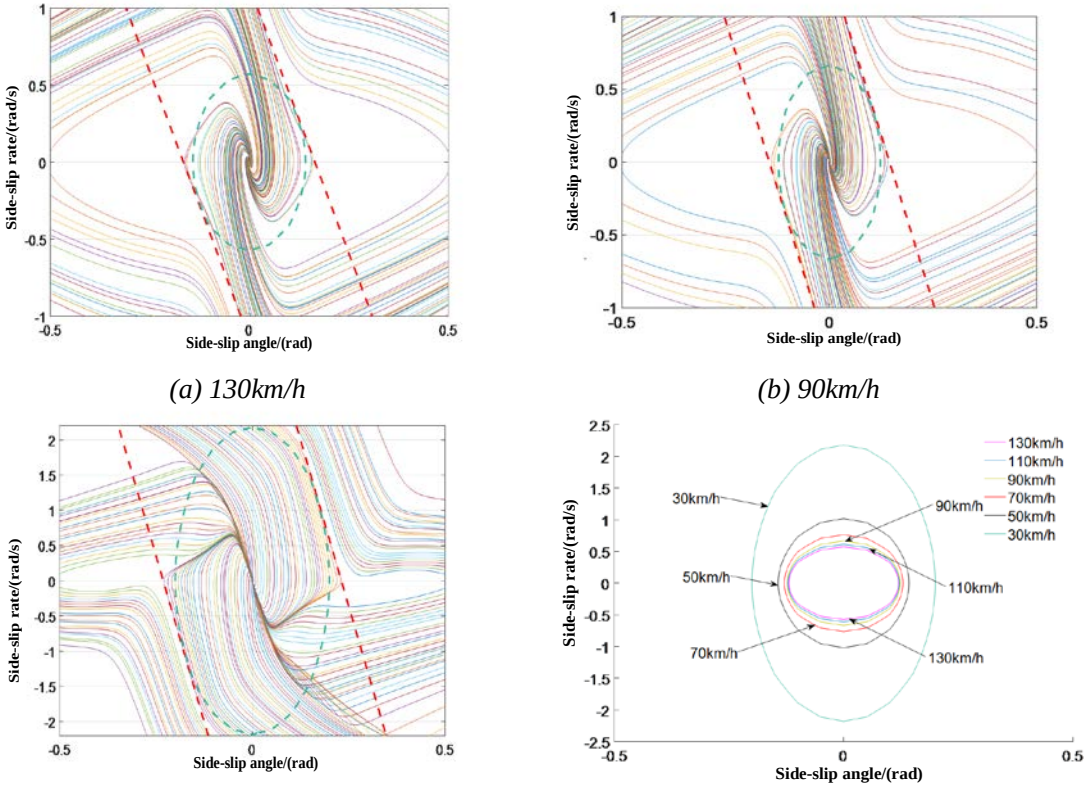

(a) 130km/h *(b) 90km/h*

(c) 30km/h *(d) Stability domain boundary*

Fig.4. *Effect of speed on phase plane boundary*

It can be seen from Fig. 4, the speed has little effect on the boundary of the phase plane stability domain, and the range of the stability domain of the phase plane at high speed is almost unchanged. When the speed is less than 30km/h, the stability domain of the phase plane is increased.

2) Effect of road adhesion coefficient on phase plane boundary

The vehicle speed is 90km/h, the front- wheel steering angle is 0^o, the range of the road adhesion coefficient μ from 0.9 to 0.1 and simulation analysis was carried at intervals of 0.1, as shown in Figure 5.

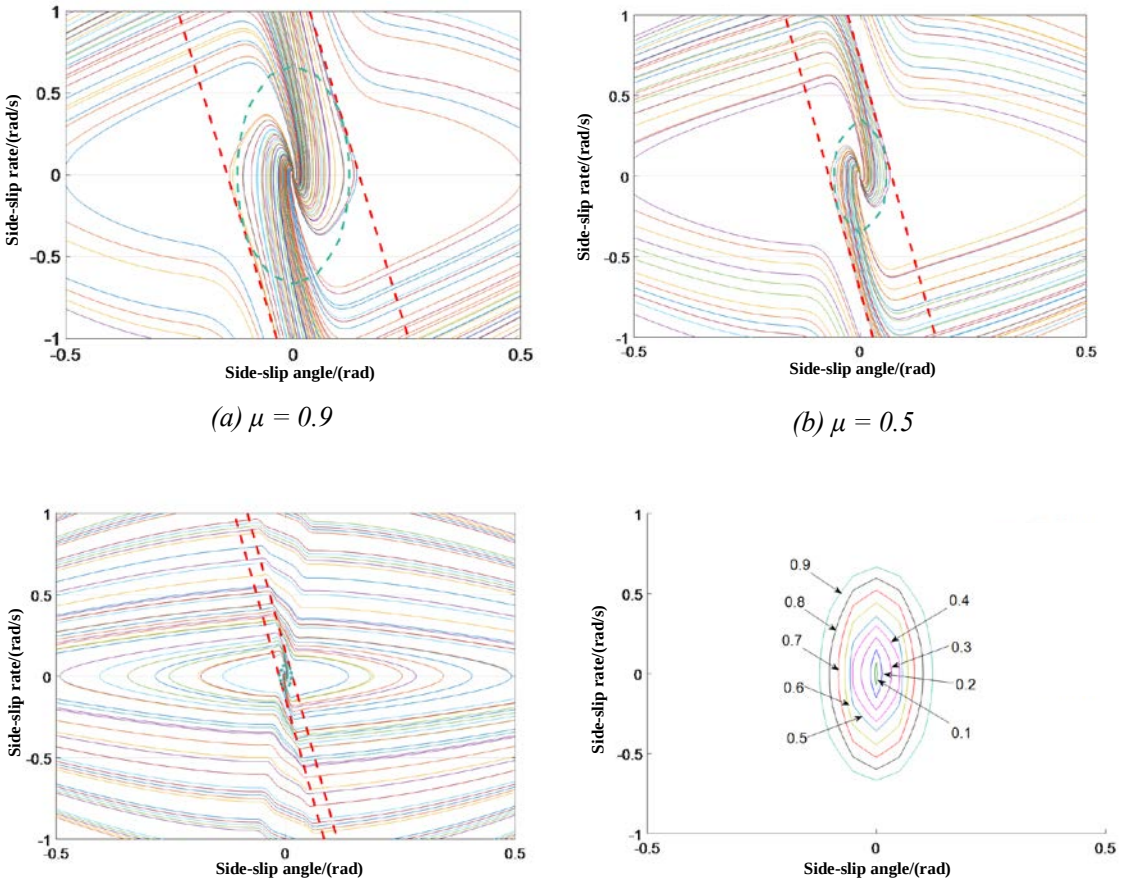

(a) μ = 0.9 *(b) μ = 0.5*

(c) μ = 0.1 *(d) Stability domain boundary*

Fig.5. Effect of road adhesion coefficient on phase plane boundary

It can be seen from Fig. 5 that the road adhesion coefficients have great effect on the boundary of the phase plane stability domain, the stability domain increases as the road surface adhesion coefficient increases.

3.2 Control System Design

There is a coupling effect between the steering system and the driving system, its performance directly affects the stability of the whole vehicle. The current research focuses on how to coordinate their control weights, so that the system performance will be optimal. Here, a vehicle integrated control strategy based on the phase plane method for the AFS and DYC systems is proposed. The layered control method is used to establish the upper, middle and lower layer controllers. The upper layer is the extension coordination controller, the middle layer is the DYC controller and the AFS controller, and the lower layer is the driving torque distribution controller for the four in-wheel-motor, as shown in Figure 6.

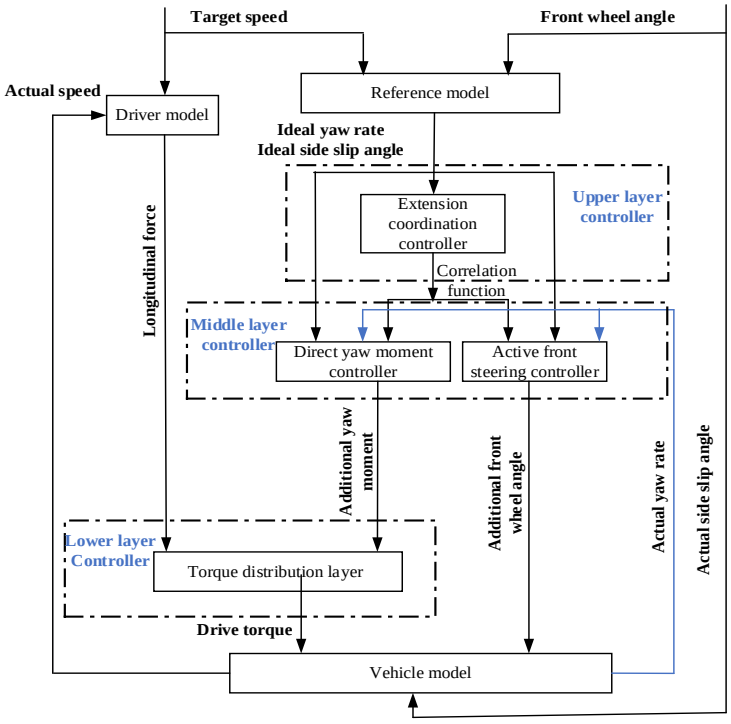

Fig.6. *Integrated control system of vehicle*

The phase plane is used to find the boundary of the stability domain. The extension coordination controller is used to obtain the correlation function between the AFS and the DYC. The extension coordination control strategy for the AFS and the DYC based on phase plane is proposed. In the extension coordination controller, the classical domain is the stability domain obtained by the phase plane. It is considered that the vehicle does not loses its stability in the classical domain, so there is no need for control in the classical domain. In the extension field, it is considered that the vehicle has a tendency to be unstable or has been slightly unstable. The AFS is adopted to improve the path tracking capability without causing a large intervention to the driver. In the non-domain, it is considered that the vehicle has begun to lose stability, and the driver cannot safely control the vehicle to run. At this time, the AFS can not keep the stable working, and the DYC is required. The DYC is adopted to ensure the vehicle stable run quickly, and the differential braking is used for compensation, both of them work together to restore the vehicle to a stable driving state.

4. Simulation Calculation and Result Analysis

In order to test the influence of the control strategy on the stability control of the whole vehicle, the simulation analysis of the double- lane change condition in which the vehicle is toward the instability during actual driving is selected. The vehicle parameters are shown in Table 1.

Table 1. *Vehicle parameters*

Parameters	Value
Mass of the vehicle $m(kg)$	1530
Vehicle moment of inertia $I_z(kg \cdot m^2)$	4607
Wheel moment of inertia $I_w(kg \cdot m^2)$	0.90
Distance from center of gravity to front	1.11
Distance from center of gravity to rear	1.67

Track width $d(m)$	1.80
Wheel rolling radius R(m)	0.28
Front tire cornering stiffness	35000
Rear tire cornering stiffness	42000
Motor parameter ξ	0.05
Peak torque of motor $T_{\dim ax}(N \cdot m)$	200
Wheel base $l(m)$	2.78
Height of the mass center $h_g(m)$	0.54
Gravity acceleration $g(m/s^2)$	9.80

In order to test the control effect of the control strategy under the ultimate state of the vehicle running, it is assumed that the road adhesion coefficient is 0.3, the speed is 70 km/h, and the simulation time is 20s. The simulation results are shown in Figure 7.

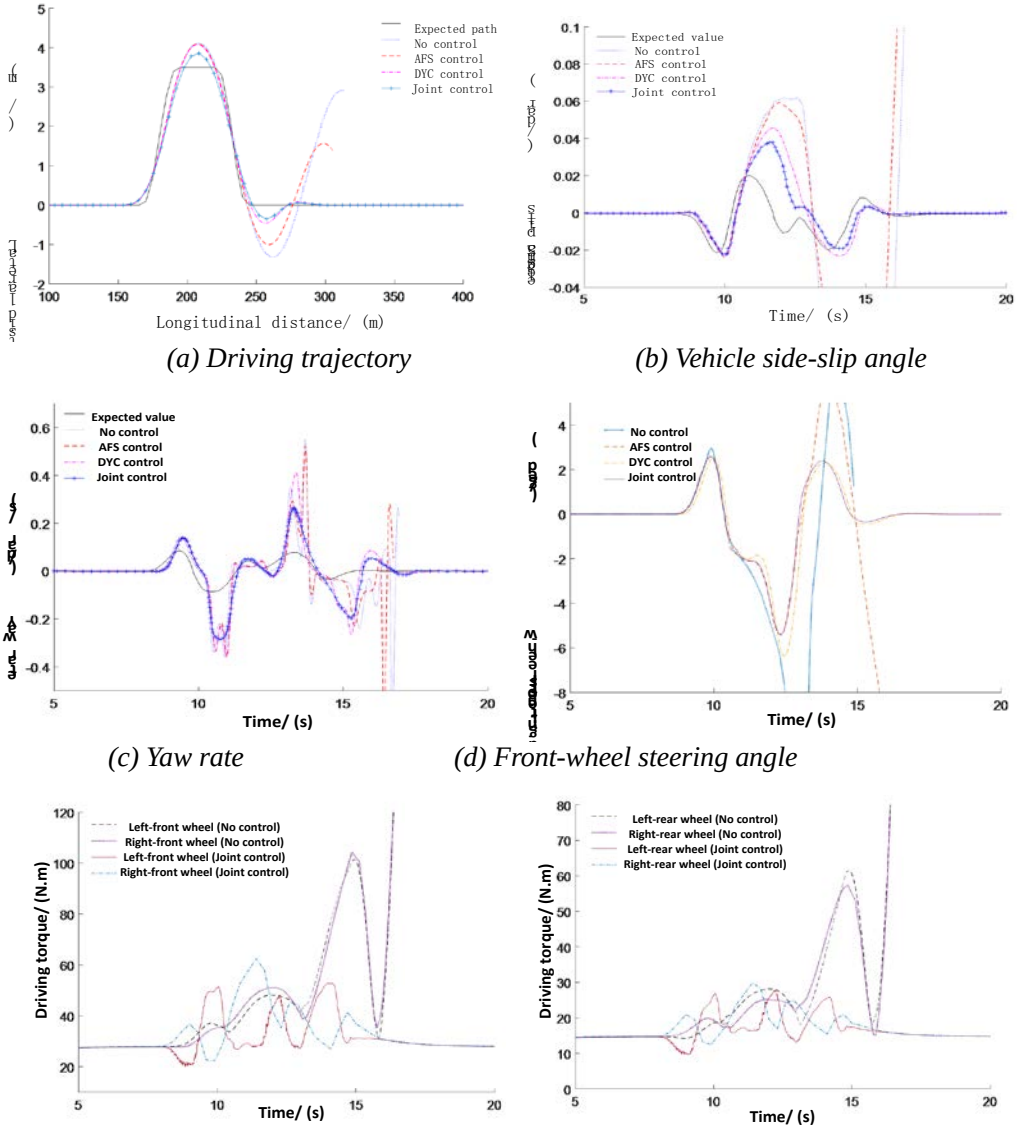

(a) Driving trajectory *(b) Vehicle side-slip angle*

(c) Yaw rate *(d) Front-wheel steering angle*

(e) Front-wheel driving torque (f) Rear-wheel driving torque

Fig.7. *Simulation results of double-shifting condition*

From Fig. 7(a) to Fig.7(c), when there is no control or the AFS controller is operated alone, the vehicle running trajectory, side-slip angle and yaw rate are seriously deviated from the expected values, indicating that the vehicle is seriously unstable at this time. When the DYC controller is used alone or the AFS and DYC

controllers are combined, the characteristic values of the vehicle stability can better track the expected values, and the extension coordination control effect reaches the best state. In Fig. 7(d), when there is no control or the AFS controller is operated alone, the front-wheel steering angle changes greatly, indicating that the vehicle is unstable. When the DYC controller is used alone or the extension coordination control is used, the front-wheel steering angle changes smoothly, indicating that the vehicle has not been unstable. From Fig. 7(e) and 7(f), when there is no control, the driving torque of the four wheels increase sharply and exceeding the torque output limit of the motor. When the extension control is combined, the torque and its change rates of the four wheels are smaller. Thus, the adoption of extension coordinatioon control has a good effect.

4. Experimental Research

4.1 Hardware-in-the-Loop Test

(1) Test platform structure

In order to verify the effect of the control method, the hardware-in-the-loop test platform was set up. The logic block diagram of the platform is shown in Fig.8.

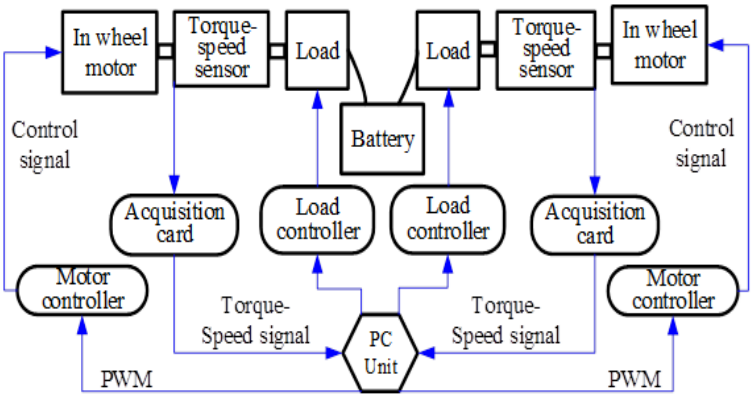

Fig.8. *Logic block diagram*

The hardware-in-the-loop simulation was implemented by CarSim-LabVIEW software, and the in-wheel-motor test platform was used to replace the Simulink model of the motor in the co-simulation. The signal of the in-wheel-motor speed is collected, and the difference between the target and actual motor speeds is calculated; then it is converted into a voltage control signal and is sent to the in-wheel-motor controller, so that the target speed is tracked and the control is achieved. At the same time, the computer collects the motor torque signal, and solves the required wheel torque values by using the vehicle controller. After converting to the voltage control signal, it is sent to the lord controller through the NI acquisition card, thereby the load value is adjusted to achieve torque control.

(2) Hardware-in-the-loop test results

The hardware-in-the-loop test was carried out under the double-lane change condition with the vehicle speed of 70 km/h and the road adhesion coefficient of 0.3. The front-wheel torque is the test data collected by the sensors during the test, and the remaining data is the output of LabVIEW model. The test results are shown in Fig.9.

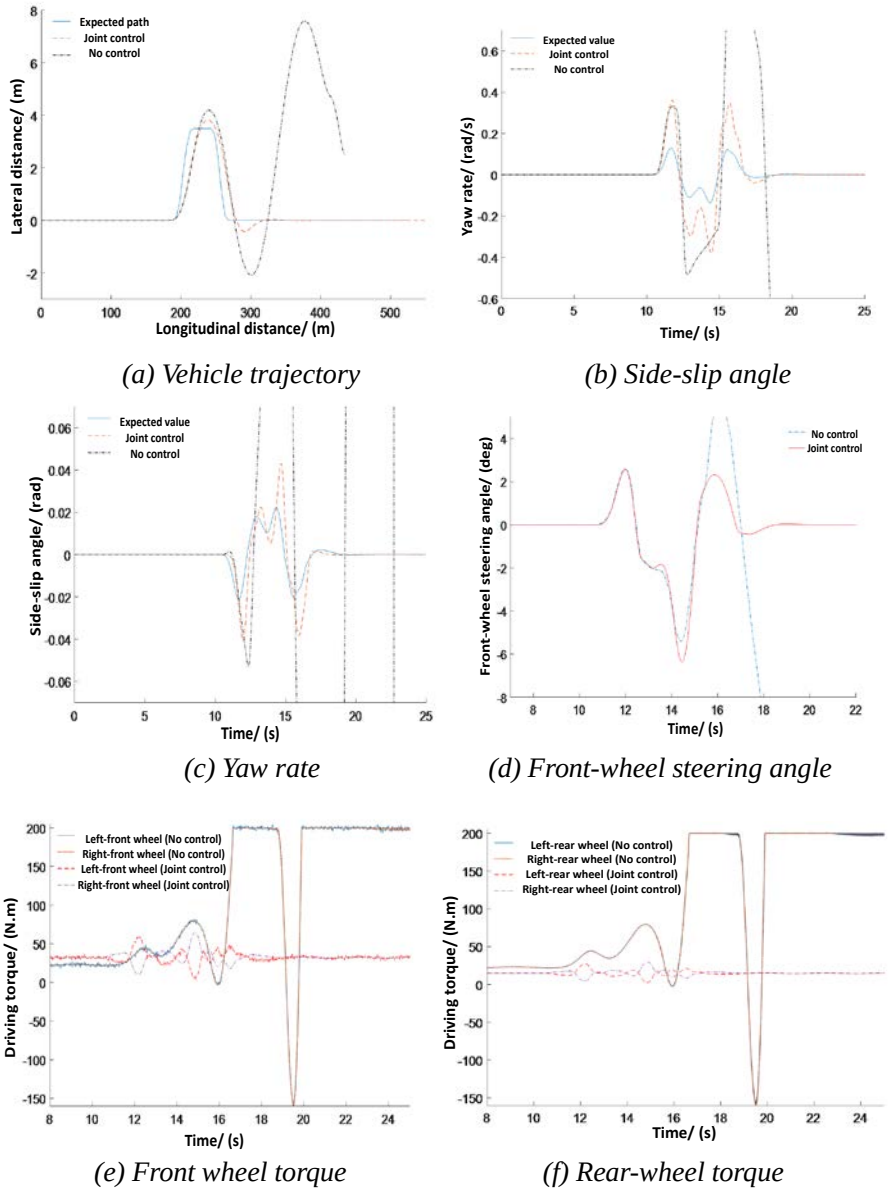

(a) Vehicle trajectory *(b) Side-slip angle*

(c) Yaw rate *(d) Front-wheel steering angle*

(e) Front wheel torque *(f) Rear-wheel torque*

Fig.9. *Hardware-in-the-loop test results*

From Figure 9(a) to (d), when there is no controller, the vehicle travelling trajectory, side-slip angle, yaw rate and front- wheel steering angle are all deviated from the expected value seriously, indicating that the vehicle is seriously unstable. However, by using the AFS and DYC extension coordinated control, the vehicle various parameters can better track the expected values, and there is no instability. The same conclusions as in the third section can be obtained from Figures 9(e) and (f).

Above all, the changing trend of the vehicle trajectory, wheel torque, side-slip angle and yaw rate can verify the control strategy validly.

5. Conclusions

1) A dynamic model of the distributed driving electric vehicle (EV) and a linear two-degree-of-freedom model are established. An extension coordination control strategy based on phase plane for the active front-wheel steering control (AFS) and the direct yaw moment control (DYC) is established.

2) The nonlinear 2-DOF model is used to draw the $\beta-\dot{\beta}$ phase plane, thus the stability domain boundary is determined, and the stability domain boundary function is fitted. Based on the phase plane, the extension coordination control strategy of the AFS and the DYC is proposed to coordinate their weights. The extension set is divided according to the stability domain boundary fitted by the phase plane method, and the weights of the AFS and the DYC controllers are calculated by the correlation function.

3) The stability simulation results of low road adhesion coefficient in the double-shifting condition by Matlab/Simulink software show that the control strategy can improve the yaw stability of the vehicle.

4) The hardware-in-the-loop (HIL) test platform was designed and implemented to test the performance of the in-wheel-motor, and the model of the in-wheel-motor based on the test data was established. The HIL test was carried out and combined with CarSim and LabVIEW software to verify the effect of the vehicle control strategy. The test results show that the control system has fast response speed and high control precision, which can effectively improve the lateral stability of the vehicle, and the riding vibration of the vehicle is also improved.

Acknowledgment

The research work was supported under National Nature Science Foundation of China (U1564201, 51675151), Scienceand Technology Major Project in Anhui Province (17030901060).

References

1. Hu S, Wang Y, Fujimoto H, et al. Robust Yaw Stability Control for In-wheel Motor
Electric Vehicles[J]. IEEE/ASME Transactions on Mechatronics, 2017, PP (99):1-1.
2. Song J. Active front wheel steering model and controller for integrated dynamics control systems[J]. International Journal of Automotive Technology, 2016, 17(2):265-272.
3. Zhang X, Göhlich D, Zheng W. Karush-Kuhn-Tuckert Based global optimization algorithm design for solving stability torque allocation of distributed drive electric vehicles[J]. Journal of the Franklin Institute, 2017.
4. Wang R, Hu C, Yan F, et al. Composite Nonlinear Feedback Control for Path Following of Four-Wheel Independently Actuated Autonomous Ground Vehicles[J]. IEEE Transactions on Intelligent Transportation Systems, 2016, 17(7):2063-2074.
5. Jun N I, Hu J, Xiang C. Envelope Control for Four-Wheel Independently Actuated Autonomous Ground Vehicle through AFS/DYC Integrated Control [J]. IEEE Transactions on Vehicular Technology, 2017, PP(99):1-1.
6. He J S. Study on the Control Strategy of Straight-ahead Driving Condition of Distributed Drive Electric Vehicle [D]. Beijing: Beijing Institute of Technology, 2015.
7. Wang J N. Study on Differential Drive Assist Steering Technology for Electric Vehicle with Independent-Motorized-Wheel-Drive[D]. Changchun: Jilin University, 2009.
8. Tan D K. Research on Key Technologies of Human-Machine Shared Lateral Driver
Assistance System [D]. Hefei: Hefei University of Technology, 2017.

9. Liu W. Vehicle Stability Control System Research Based on Side-slip Angle Phase
[D]. Changchun: Jilin University, 2013.